*Computers Math. Applic.* Vol. 18, No. 10/11, pp. 883–892, 1989
Printed in Great Britain

0097-4943/89 $3.00 + 0.00
Maxwell Pergamon Macmillan plc

# A COMPARTMENTAL REACTION-DIFFUSION CELL CYCLE MODEL†

S. N. BUSENBERG
Department of Mathematics, Harvey Mudd College, Claremont, CA 91711, U.S.A.

J. M. MAHAFFY
Department of Mathematical Sciences, San Diego State University, San Diego, CA 92182, U.S.A.

## 1. INTRODUCTION

Before a typical cell can divide it must double its mass and duplicate its contents so that the new daughter cells can contain the components needed for independent growth and eventual division. Most of these components are made continuously throughout the cell cycle with the striking exception of DNA whose synthesis occurs during a restricted period, the so called *S phase*, of the cell cycle. The *S phase* is preceded by the $G_1$ *phase* whose time length is the main determinant of the length of the cycle [1]. The mechanism that determines the initiation of the *S phase*, hence, the end and length of the $G_1$ *phase*, is important in setting the reproduction time of the cell but has eluded a definitive experimental determination. Consequently, a number of models have been proposed to explain this mechanism (see Winfree [2, Chap. 13] for a stimulating review, and Alberts *et al.* [1, Chap. 11], for a more recent overview). One of the early models of this type, due to Goodwin [3, 4], relates the cell cycle time to the period of the epigenetic oscillations that can occur in a nonlinear system controlled by negative feedback. This model is based on the well-established theory of Jacob and Monod [5] for genetic control of biosynthetic pathways by repression. The periods of these epigenetic oscillations have been found to be too short to account for the cell cycle (see Banks and Mahaffy [6]), however, the possibility of finding a basis for the triggering of the *S phase* in such a well established biochemical process in the cell is quite appealing. In Busenberg and Mahaffy [7] we have presented and analyzed such a model for a possible triggering mechanism. Here we shall describe this model, review the results we have obtained in both Refs [7, 8], and give some of the analysis and new results that lend support to it.

Our model is related to Goodwin's [3, 4] in that it is based on the generation of epigenetic oscillations due to genetic control by repression. However, unlike Goodwin's proposed mechanism, in our model, it is not the periods of these oscillations that determine the cell cycle time. Rather, it is an intricate coupling between the size and shape of the growing cell and the biochemical reaction-diffusion processes in the cell that determines the initiation of the epigenetic oscillations, hence, the $S_1$ *phase* triggering mechanism. We present the model in its simplest possible version where there are just two interacting biochemical species in the process of control by repression since the suggested origin of the triggering mechanism is most clearly evident in this setting. This simplification is valid because the same triggering mechanism still operates in more realistic cases involving long chains of biochemical reactions that lead to end-product control by repression.

The model we propose considers the eukaryotic cell as a system consisting of two compartments, the nucleus and the cytoplasm, where basic biochemical processes occur. In the cytoplasmic compartment we assume that the reactants diffuse, while in the smaller nucleus, we assume that the reactions occur as in a well-mixed compartment. We consider a two component reaction (say mRNA and an end-product repressor) with the repressor production being stimulated by the mRNA in the cytoplasm, while the mRNA production in the nucleus is inhibited by the presence of the end product repressor. The time delays involved in the processes of transcription and translation are included in the model.

The triggering mechanism that we propose involves the destabilization, caused by the growth of the cell of the steady-state concentrations of the two biochemical components leading to

†To avoid further delay, this paper has been published without the authors' corrections.

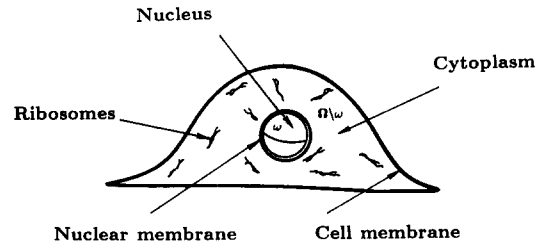


Fig. 1. The two compartment eukaryotic cell model.

time-periodic oscillatory concentrations. The peak levels of these oscillating concentrations are much higher than the steady-state levels thus possibly triggering either a gradient or a critical level sensor in the cell that signals the initiation of DNA synthesis. In fact, we shall show that as the cell grows, the reaction-diffusion equations of our two compartment model undergo a change in stability which initiates these oscillatory solutions.

The model we treat is presented in Ref. [7]. The basic equations of the model are given in Refs [7, 8] and are based on a generalization of an earlier model for epigenetic oscillations that is derived in Mahaffy and Pao [9]. The specific model pictured in Fig. 1 consists of two separate compartments enclosed within the cell wall and separated by a permeable nuclear membrane.

The first compartment, labeled $\omega$ in the figure, represents the nucleus where mRNA is produced in a setting approximating a well-mixed chemical reactor. The second compartment denoted by $\Omega\backslash\omega$ represents the cytoplasm in which the end-product repressor is produced at the randomly dispersed ribosomes. The interaction between the two compartments occurs through the processes of diffusion in the cytoplasm and transfer proportional to concentration gradients through the membrane bounding the nucleus. Let $u_i$ and $v_i$, $i = 1, 2$, denote the concentration of mRNA and repressor, respectively, in compartments $\omega$ for $i = 1$, and $\Omega\backslash\omega$ for $i = 2$. Then our model takes the form shown in the following system of equations:

$$\begin{aligned}
\dot{u}_1(t) &= f(v_1(t - v_1)) - b_1 u_1(t) + \gamma_1 \int \partial\omega\ [u_2(x, t) - u_1(t)]\, \mathrm{d}S_\omega, \\
\dot{v}_1(t) &= -b_2 v_1(t) + \gamma_2 \int \partial\omega\ [v_2(x, t) - v_1(t)]\, \mathrm{d}S_\omega, \\
\frac{\partial u_2(x, t)}{\partial t} &= \mu_1 \nabla^2 u_2(x, t) - b_1 u_2(x, t), \quad x \in \Omega\backslash\omega, \\
\frac{\partial v_2(x, t)}{\partial t} &= \mu_2 \nabla^2 v_2(x, t) - b_2 v_2(x, t) + c_0 u_2(x, t - v_2), \quad x \in \Omega\backslash\omega,
\end{aligned} \tag{1.1}$$

with boundary conditions

$$\begin{aligned}
\frac{\partial u_2(x, t)}{\partial n} &= -\beta_1 [u_2(x, t) - u_1(t)], \quad x \in \partial\omega, \\
\frac{\partial v_2(x, t)}{\partial n} &= -\beta_1^* [v_2(x, t) - v_1(t)], \quad x \in \partial\omega, \\
\frac{\partial u_2(x, t)}{\partial n} &= \frac{\partial v_2(x, t)}{\partial n} = 0, \quad x \in \partial\Omega.
\end{aligned} \tag{1.2}$$

The constants $b_i$ are the kinetic rates of decay, $a_i$ are the transfer rates between the compartments, and $c_0$ is the rate constant for production of the repressor. All biochemical species are presumed to decay at a rate proportional to their concentrations either through degradation or dilution. One particular form of the feedback control term that we consider is $1/[1 + kv_1^\rho(t - v_1)]$, where $v_1 \geqslant 0$ represents the delay from transcription, $k$ is a kinetic constant, and $\rho$ is the Hill coefficient. Obviously, this model is an over-simplification of the actual biochemical processes involved in repression, yet it satisfies the generic qualities of a negative feedback system. A detailed discussion of this type of repression control model can be found in Banks and Mahaffy [6], Goodwin [4] and Tyson [10].

In our model, as the cell grows, equations (1.1) undergo a change of stability. Throughout most of the growth part of the cell cycle the biochemical concentrations $u_i$ and $v_i$ remain at an equilibrium level. However, at a critical cell diameter which depends on the various kinetic constants as well as on the transcription and translation delays, the equilibrium concentrations become unstable and begin oscillating. The oscillating concentrations increase in peak amplitude and trigger either a gradient or a critical level sensor in the cell signalling the start of DNA synthesis. This is our proposed triggering mechanism for the start of the *S phase*.

In order to clearly present the implications of these results on cell timing, we first give the main numerical results we have obtained in the special idealized case where the cell and its nucleus are spherically shaped, and in the repression term the Hill coefficient $\rho = 4$. The restriction to spherical shapes was made in order to simplify the computations which are quite time consuming. Further work on different shaped cells is currently being done and will be described in Section 3. Figures 2 and 3 show the curves separating the regions of stable equilibrium concentrations from the regions where the oscillatory solutions exists.

The pertinent three parameters are the volume of the cell, the sum $v = v_1 + v_2$ of the transcription and translation delays, and the ratio $\sigma$ of the nuclear diameter to the cell diameter. Consider a fixed value of the delay $v$ and of the aspect ratio $\sigma$. As the radius of the cell increases from an initial size $R_0$ to a final size $R_1$ it crosses the critical size $R_c$ where the oscillatory solutions begin. On further growth, the amplitudes of these oscillations increase until at size $R_1$ they exceed the threshold levels necessary for the triggering of DNA synthesis. At this stage, the cell continues through the rest of its cycle, ending up with two daughter cells of initial size $R_0$, and the process starts again for each of these daughter cells. This triggering mechanism does not require any contrived forces or outside effects and is based on established biochemical and physical processes. It is affected by environmental or internal factors that change the growth rate, shape, and the reaction and transfer constants of the cell. It is interesting to note that, according to our results, if a cell grows beyond a given fixed size yet avoiding the initiation of DNA synthesis, then it returns to a stable concentration situation and may not complete its normal division cycle. The reader may wish to compare this type of mechanism to two other recently proposed and analyzed mechanism for cell cycle control found in Lasota and Mackey [11], Mackey [12] and Alt and Tyson [13].

In the next section we start with a description of our mathematical analysis of this model and a detailed study of the dependence of the critical stability curve when the diffusion rates are varied as well as when the cell is viewed as a three-, two- and one-dimensional spatial domain. The models of the cell as a two- and one-dimensional domain are of interest since they show some of the effects that cell shape can have on the critical stability region. We then present our results on the dependence of the critical stability curve on the cell volume. These results form the basis for the triggering mechanism that we have presented above. In the final section we discuss extensions of the work on the current models as well as more elaborate models that we are currently pursuing.

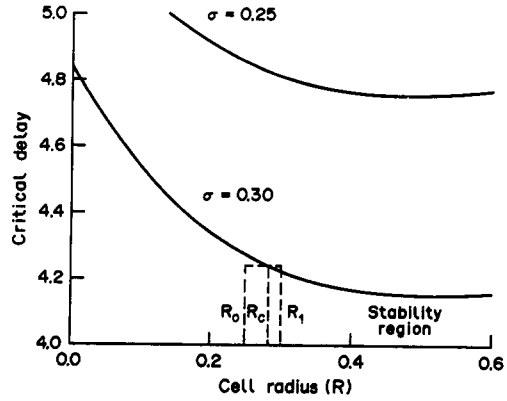


Fig. 2. Dependence of the stability region on the cell diameter and the delay.

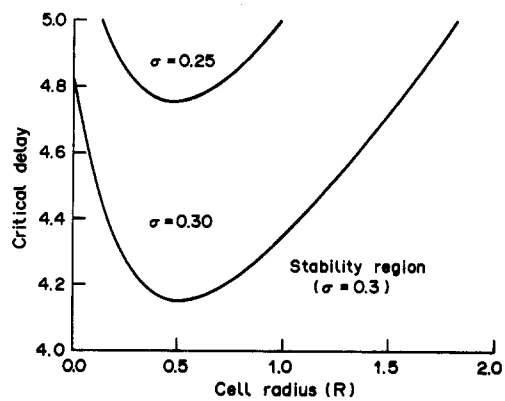


Fig. 3. Dependence of the stability region on the cell diameter and the delay.

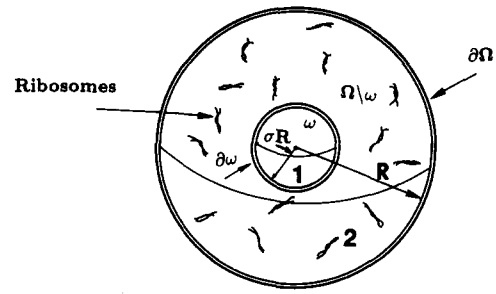


Fig. 4. Concentric sphere model of the two-compartment cell.

## 2. MATHEMATICAL ANALYSIS AND RESULTS

In Fig. 4 we depict the simple case of the model where the cell is spherically symmetric. The model as diagrammed in Fig. 4 is derived and analyzed in Ref. [8] and is based on a one-dimensional model introduced by Mahaffy and Pao [9]. The first compartment labeled $\omega$ consists of the cell nucleus, and the second compartment denoted $\Omega\backslash\omega$ consists of the cell interior minus the nucleus. If $u_i$ and $v_i$, $i = 1, 2$, denote the concentrations of mRNA and repressor respectively in the two compartments, then the repression model is given by the system of equations (1.1) and (1.2).

To perform a detailed analysis of this model we examine the specific cases of one-, two- and three-dimensional models with symmetric geometries, such as concentric spheres in the three-dimensional case. The cell radius is given by $R$ and the inner radius is given by $r = \sigma R$ as shown in Fig. 4. A change of variables is made to make the system of equations (1.1) dimensionless and shift the delay into the nonlinear function $f$ only. Furthermore, the unique, radially symmetric, steady-state solution $(\bar{u}_1, \bar{v}_1, u_2^s, v_2^s)$ is computed for the model, then the system of equations is translated about the steady-state solution in a way that renders the boundary conditions homogeneous. With this change of variables we find that the system of equations (1.1) can be written as follows:

$$\dot{u}(\tau) = f(v_1(\tau - \nu) + \bar{v}_1) - u_1(\tau) + \gamma_1 u_2(\sigma, \tau) + \gamma_1 u_2^s(\sigma) - (1 + \gamma_1)\bar{u}_1 \equiv F_1(u_1(\tau), v_{1\tau}, u_2(\phi, \tau)),$$

$$\dot{v}_1(\tau) = -b_2 v_1(\tau) + \gamma_2 v_2(\sigma, \tau) \equiv G_1(v_1(\tau), v_2(\sigma, \tau)),$$

$$\frac{\partial u_2(r, \tau)}{\partial \tau} = \mu_1 \nabla^2 u_2(r, \tau) - u_2(r, \tau) - u_1(\tau) - F_1(u_1(\tau), (v_{1\tau}, u_2(\sigma, \tau)),$$

$$\equiv \mu_1 \nabla^2 u_2(r, \tau) - u_2(r, \tau) - F_2(v_{1\tau}, u_2(\sigma, \tau)),$$

$$\frac{\partial v_2(r, \tau)}{\partial \tau} = \mu_2 \nabla^2 v_2(r, \tau) - b_2[v_2(r, \tau) + v_1(\tau)] + c_0[u_2(r, \tau) + u_1(\tau)] - G_1(v_1(\tau), v_2(\sigma, \tau))$$

$$\equiv \mu_2 \nabla^2 v_2(r, \tau) - b_2 v_2(r, \tau) - G_2(u_1, u_2(r, \tau), v_2(\sigma, \tau)), \tag{2.1}$$

with boundary conditions

$$\frac{\partial u_2(\sigma, \tau)}{\partial r} = \beta_1 u_2(\sigma, \tau), \quad \frac{\partial v_2(\sigma, \tau)}{\partial r} = \beta_1^* v_2(\sigma, \tau)$$

and

$$\frac{\partial u_2(1, \tau)}{\partial r} = \frac{\partial v_2(1, \tau)}{\partial r} = 0.$$

At this point we have a complicated system of differential equations. The first two equations are delay-differential equations in $u_1$ and $v_1$ which, in addition to their dependence on $u_1$ and $v_1$, depend on the values that $u_2$ and $v_2$ assume on the boundary separating the two compartments. The second two equations have become more complicated by the change of variables, but they have homogeneous boundary conditions. Closer inspection of the third equation shows that the function

$F_1$ depends only on $u_2$ along the boundary and on $v_1$ which is only a time dependent function. This suggests the variation of constants technique which we outline below.

To proceed with the more detailed analysis we utilize the radial symmetry to form a problem with separable variables. For the $u_2$ equation we examine the linear problem:

$$\frac{\partial u_2}{\partial t} = \mu_1 \nabla^2 u_2 - u_2,$$

with boundary conditions

$$\frac{\partial u_2(\sigma, \tau)}{\partial r} - \beta_1 u_2(\sigma, \tau) = 0 \quad \text{and} \quad \frac{\partial u_2(1, \tau)}{\partial r} = 0,$$

where

$$\nabla^2 = (1/\tau^{n-1})\, \partial[r^{n-1}\, \partial/\partial r]\, \partial r$$

and $n = 1, 2$ and 3 depending on the dimension of the system. Considering the spatial part of the separable problem we find the eigenvalues and associated eigenfunctions. The eigenvalues $\lambda$ satisfy:

$$\cot(\lambda) - \lambda/\beta_1 = 0,$$

$$\lambda[J_1(\lambda\sigma)Y_1(\lambda) - J_1(\lambda)Y_1(\lambda\sigma)] - \beta_1[J_1(\lambda)Y_0(\lambda\sigma) - J_0(\lambda\sigma)Y_1(\lambda)] = 0,$$

$$(\lambda^2\sigma + 1)\sin\lambda(1-\sigma) - \lambda(1-\sigma)\cos\lambda(1-\sigma) - \beta_1\sigma(\lambda\cos\lambda(1-\sigma) - \sin\lambda(1-\sigma)) = 0, \quad (2.2)$$

in one, two, and three dimensions, respectively. The corresponding eigenfunctions $\phi_n$ are given by:

$$\phi_n(r) = \frac{2\sqrt{\lambda_n}\cos(\lambda_n r)}{\sqrt{2\lambda_n + \sin(2\lambda_n)}},$$

$$\phi_n(r) = \frac{\pi\lambda_n\sqrt{2}[Y_1(\lambda_n)J_0(\lambda_n r) - J_1(\lambda_n)Y_0(\lambda_n r)]}{[4 - \sigma^2\pi^2(\lambda_n^2 + \beta_1^2)(J_0(\lambda_n\sigma)Y_1(\lambda_n) - J_1(\lambda_n)Y_0(\lambda_n\sigma))^2]^{1/2}},$$

$$\phi_n(r) = \frac{2\sqrt{\lambda_n}(\lambda_n\cos\lambda_n(1-r) - \sin\lambda_n(1-\tau))}{r[(\lambda_n^2+1)(2\lambda_n(1-\sigma)) - 2\lambda_n + 2\lambda_n\cos 2\lambda_n(1-\sigma) + (\lambda_n^2-1)\sin 2\lambda_n(1-\sigma)]^{1/2}}. \quad (2.3)$$

in one, two, and three dimensions, respectively.

Having found the eigenfunctions to the linear part of the partial differential equation in equations (2.1), a variation of constants formula can be used to find the solution $u_2(r, \tau)$. Let $A_n = 1 + \lambda_n^2\mu_1$, $\delta_n = \langle\phi_n, 1\rangle$, and $a_n = \langle u_{20}, \phi_n\rangle$, where $u_{20}(r) = u_2(r, 0)$ and $\langle f, g\rangle = \int_0^1 f(r)g(r)r^{n-1}\,dr$, $n$ being the dimension of the problem. With these definitions, the variation of constants formula applied to the $u_2$ equation in equations (2.1) yields:

$$u_2(r, \tau) = \sum_{n=1}^{\infty} \alpha_n e^{-A_n\tau}\phi_n(r) - \int_0^{\tau}\sum_{n=1}^{\infty}\delta_n\phi_n(r)e^{-A_n(\tau-s)}F_2(s)\,ds$$

$$\equiv \sum_{n=1}^{\infty}\alpha_n e^{-A_n\tau}\phi_n(r) - \int_0^{\tau} K(\tau - s, r)[\tilde{f}(v_1(s-v)) + \gamma_1 u_2(\sigma, s)]\,ds,$$

where $K(\tau, r) = \Sigma_{n=1}^{\infty}\delta_n\phi_n(r)e^{-A_n\tau}$ and $\tilde{f}(v_1(s-v)) = f(v_1(s-v) + \bar{v}_1) + \gamma_1 u_2^s(\sigma) - (1+\gamma_1)\bar{u}$.

We integrate the above equation along the boundary $\omega$ and find a linear Volterra equation for $u_2$ along the boundary of $\omega$ which, in the radially symmetric cases that we are examining, reduces to the following:

$$u_2(\sigma, \tau) = \sum_{n=1}^{\infty}\alpha_n e^{-\lambda_n\tau}\phi_n(\sigma) - \int_0^{\tau} K(\tau - s, \sigma)[\tilde{f}(v_1(s-v)) + \gamma_1 u_2(\sigma, s)]\,ds.$$

A similar procedure can be applied to the $v_2$ equation. If we let $\zeta_n$ and $\psi_n(r)$ be the eigenvalues and eigenfunctions for the linear part of the $v_2$ equation and define $B_n = b_2 + \zeta_{\mu 2}$, $\delta_n^* = \langle\psi_n, 1\rangle$, $\alpha_n^* = \langle v_{20}, \psi_n\rangle$ and $K^*(\tau, r) = \Sigma_{n=1}^{\infty}\delta_n^* e^{B_n\tau}\psi_n(\tau)$, then the linear Volterra equation for $v_2$ can be

found. Combining this information with our equation for $u_2$, we can write the following system of delay differential equations and linear Volterra equations:

$$u_1'(\tau) = \tilde{f}(v_1(\tau - v)) - u_1(\tau) + \gamma_1 u_2(\sigma, \tau),$$

$$v_1'(\tau) = -b_2 v_1(\tau) + \gamma_2 v_2(\sigma, \tau),$$

$$u_2(\sigma, \tau) = \sum_{n=1}^{\infty} \alpha_n e^{-A_n \tau} \phi_n(\sigma) - \int_0^{\tau} K(\tau - s, \sigma)[\tilde{f}(v_1(s - v)) + \gamma_1 u_2(\sigma, s)]\, ds$$

$$v_2(\sigma, \tau) = \sum_{n=1}^{\infty} \alpha_n^* e^{-B_n \tau} \psi_n(\sigma) + \int_0^{\tau} K^*(\tau - s, \sigma)[c_0 u_1(s) - \gamma_2 v_2(\sigma, s)]\, ds$$

$$+ c_0 \int_0^{\tau} \sum_{n=1}^{\infty} e^{-B_n(\tau - s)} \psi_n(\sigma) < u_2(\cdot, s), \psi_n(\cdot) > ds. \tag{2.4}$$

The above system of differential equations is significant as its only spatial component in the part containing the initial conditions and this part is exponentially damped with increasing time. Thus we have reduced a system of delay-partial differential equations to a system of delay differential equations and linear Volterra equations which are essentially only time dependent. This naturally leads us to the use of techniques for analysis of time dependent equations. We linearize equations (2.4) and find the limiting Volterra equations as follows:

$$u_1'(\tau) = f'(\bar{v}_1) v_1(\tau - v) - u_1(\tau) + \gamma_1 u_2(\sigma, \tau),$$

$$v_1'(\tau) = -b_2 v_1(\tau) + \gamma_2 v_2(\sigma, \tau),$$

$$u_2(\sigma, \tau) = -\int_0^{\infty} K(\tau - s, \sigma)[f'(\bar{v}_1) v_1(s - v) + \gamma_1 u_2(\sigma, s)] ds,$$

$$v_2(\sigma, \tau) = \int_0^{\infty} [K^*(\tau - s, \sigma)[c_0 u_1(s) - \gamma_2 v_2(\sigma, s)]$$

$$- c_0[f'(\bar{v}_1) v_1(s - v) + \gamma_1 u_2(\sigma, s)] \sum_{n=1}^{\infty} \mathcal{K}_n(\tau - s)]\, ds, \tag{2.5}$$

where $\mathcal{K}_n(s) = \psi_n(\sigma) \int_0^s e^{-B_n t} < K(s - t, \cdot), \psi_n(\cdot) > dt$.

Now, fairly standard methods can be employed to obtain the characteristic equation for equations (2.5). For clarity of argument, we shall present only the case when $\beta_1 = \beta_1^*$. By expanding the $4 \times 4$ determinant which yields the spectrum of equations (2.5), and integrating out the Volterra kernels, the characteristic equation takes the following form:

$$(\lambda + 1)\left[\lambda + 1 + \lambda_1^2 \mu_1 + \gamma_1 \delta_1 \phi_1(\sigma) + \gamma_1 \sum_{n=2}^{\infty} \frac{\delta_n \phi_n(\sigma)(\lambda + 1 + \lambda_1^2 \mu_1)}{\lambda + 1 + \lambda_n^2 \mu_1}\right]$$

$$x(\lambda + b_2)\left[\lambda + b_2 + \lambda_1^2 \mu_2 + \gamma_2 \delta_1 \phi_1(\sigma) + \gamma_2 \sum_{n=2}^{\infty} \frac{\delta_n \phi_n(\sigma)(\lambda + b_2 + \lambda_1^2 \mu_2)}{\lambda + b_2 + \lambda_n^2 \mu_2}\right] - c_0 \gamma_2 f'(\bar{v}_1) e^{-\lambda v}$$

$$\times \left[\lambda_1^2 \mu_1 \delta_1 \phi_1(\sigma) + \sum_{n=2}^{\infty} \frac{\delta_n \phi_n(\sigma) \lambda_n^2 \mu_1 (\lambda + 1 + \lambda_1^2 \mu_1)(\lambda + b_2 + \lambda_1^2 \mu_2)}{(\lambda + 1 + \lambda_n^2 \mu_1)(\lambda + b_2 + \lambda_n^2 \mu_2)}\right] = 0. \tag{2.6}$$

This characteristic equation is rather complicated, but there are techniques for analyzing this equation, as we shall see below.

Before proceeding with the analysis we compare the characteristic equation (2.6) to the characteristic equation of a related model where the second compartment is well-mixed. This model is given by:

$$\begin{aligned}
\dot{u}_1(t) &= f(v_1(t-v)) - u_1(t) + a_1(u_2(t) = u_1(t)),\\
\dot{v}_1(t) &= -b_2 v_1(t) + a_2(v_2(t) - v_1(t)),\\
\dot{v}_2(t) &= -u_2(t) + a_3(u_1(t) - u_2(t)),\\
\dot{v}_2(t) &= c_0 u_2(t) - b_2 v_2(t) + a_4(v_1(t) - v_2(t)),
\end{aligned} \tag{2.7}$$

and its characteristic equation can be shown to have the following form:

$$(\lambda + 1)(\lambda + b_2)(\lambda + 1 + a_1 + a_3)(\lambda + b_2 + a_2 + a_4) - c_0 a_2 a_3 f'(\bar{v}_1)\mathrm{e}^{-\lambda v} = 0. \tag{2.8}$$

If the infinite sums in equation (2.6) are shown to tend to zero as the diffusivities become large, then there is a clear correlation between equations (2.6) and (2.8). In fact one can demonstrate the following theorem.

*Theorem 2.1*

Assume that the diffusion rates $\mu_i$ tend to infinity and $\beta_1\mu_1$ and $\beta_1^*\mu_2$ are finite. Consider $\lambda$ such that $\operatorname{Re}\lambda > \max(-1, -b_2)$. Then, in the limit, the solutions $\lambda$ which satisfy the characteristic equation (2.6) for the model (2.1) equal the solutions $\lambda$ to the characteristic equation (2.8) for the well-mixed two compartment model (2.7) with $\gamma_1 = a_1$, $\gamma_2 = a_2$, $\beta_1\mu_1 = a_3$, and $\beta_1^*\mu_2 = a_4$.

This theorem proves that, as one would expect, the diffusion model has behavior similar to the well-mixed model when the diffusivities are large. A more surprising result is that when the diffusivities are small there is a region of asymptotic stability. The physical argument for a theorem of this type is that if the diffusivity is sufficiently small, then the chemical species cannot diffuse far enough into the second compartment and react before the chemical breaks down. The theorem describing the result is given by the following.

*Theorem 2.2*

Suppose the $\beta_1\mu_1 = a_3$, $\beta_1^*\mu_2 = a_4$, with $a_3$, $a_4$ fixed and suppose that $\mu_1$, $\mu_2$ tend to zero. Then there exists $d > 0$ such that if $0 < \mu_i < d$, all solutions $\lambda$ which satisfy the characteristic equation (2.6) have real parts less than zero.

Details of the proofs of these theorems can be found in Ref. [8].

The analysis for a characteristic equation of the form in equation (2.8) has been developed in Mahaffy [14]. One can readily see that equation (2.8) can be written in the form:

$$P(\lambda) + Q(\lambda)\mathrm{e}^{-\lambda v} = 0, \tag{2.9}$$

where $P(\lambda)$ is a polynomial with all real negative roots and $Q(\lambda)$ is a constant. It was shown in Ref. [14] that if $P(0) < Q(0)$, then there exists a unique critical delay $v^*$ for which the differential equation from which equation (2.9) was derived loses stability for all $v > v^*$. The method for showing this Hopf bifurcation uses the "argument principle" from complex variables. To actually compute this bifurcation one simply finds an $\omega^*$ such that $|P(i\omega^*)| = |Q(i\omega^*)|$ (by a bisection method), then the critical delay is found by the formula:

$$v_0 = \frac{\pi + \arg[Q(i\omega^*)] - \arg[P(i\omega^*)]}{\omega^*}. \tag{2.10}$$

The argument employed in Ref. [14] is geometric and can handle perturbations. We treat equation (2.6) as a perturbation of the well-mixed case, where functions $P(\lambda)$ and $Q(\lambda)$ are now the more complicated expressions involving infinite sums. Still we find an $\omega^*$ by the bisection method for which $|P(i\omega^*)| = |Q(i\omega^*)|$, then the critical delay is given by equation (2.10) for the model with diffusion and delays.

With the technique described above applied to equation (2.6), using the eigenvalues computed in equations (2.2) and the eigenfunctions computed in equation (2.3), we can find the critical delay

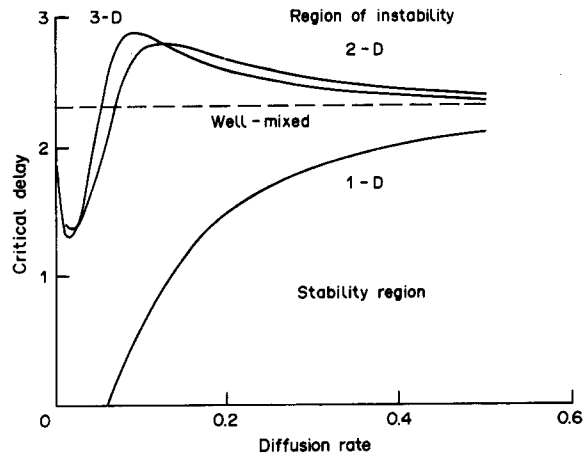


Fig. 5. Dependence of the stability region on the diffusion rate and the delay.

versus the diffusivity curve for one, two and three dimensions. These results are presented below in Fig. 5. Note that for these computations the diffusivities are taken to all be the same. In addition, the other kinetic constants are scaled appropriately so that the mass balance of the different dimensions agree with the well-mixed model for a fixed volume ratio of 1:25 for the first compartment to the second compartment.

In Fig. 5 for one dimension, we observe the predicted behavior that, as the diffusivity decreases, the time delay necessary to destabilize the system of delay differential-Volterra equations decreases. Intuitively, this agrees with the reasoning in MacDonald [15] that diffusion acts as a time delay. In fact, the graph shows that for a diffusivity near 0.06 the system becomes unstable without any delays in the equations. The graph does not consider diffusivity values sufficiently small for the effect of Theorem 2.2 to be seen in one dimension. However, in two and three dimensions the graphs are seen to show the opposite effect initially as the diffusivity is decreased. There is some local maximum value of the critical delay which is reached before the graphs turn sharply downward and give the behavior of an additional delay. This behavior has not been explained to date. The curves for two and three dimensions show the beginning of the behavior described in Theorem 2.2 for very low diffusivities. Numerically, the computations require increasing amounts of computer time as the diffusivity decreases since the number of terms in the infinite sums necessary for accurate estimates increases.

We now turn to the two- and three-dimensional models and discuss the result which connects cell size with the triggering mechanism.

*Theorem 2.3*

For both the two- and three-dimensional model with central symmetry, suppose that $\beta_1 \mu_1 = a_3 R$ and $\beta_1^* \mu_2 = a_4 R$. Then there exists a constant $M > 0$ such that if $R > M$ all solutions of the characteristic equation (2.6) have real parts less than zero.

The result shows that, regardless of the size of the transcription and translation delays, the steady state concentrations will be stable for large enough cell radii $R > M$. The detailed stability boundary is determined by numerically solving the characteristic equation in this case and is shown in a sample case in Fig. 3. Note that the cut-off values of the cell size above which stability prevails are evident in the data plotted in that figure. It is easy to find parameters for which the bifurcation curve initially decreases, giving the shape necessary for the proposed triggering mechanism.

In Theorem 2.8, the flux rate per unit surface area is kept fixed while the cell radius is changing. The cell volume increases by a factor $R$ times surface, the transfer rate through the nuclear membrane which is proportional to its area becomes relatively small for $R$ large enough and the feedback induced oscillations cannot be mainained for such $R$.

The proofs of these results are given in Ref. [7] and are based on a detailed analysis of the characteristic equations (2.6) and (2.8) for the two- and three-dimensional models. Note that Theorem 2.1 connects the characteristic equations (2.6) and (2.8) when the diffusion rates are large. The comparable result for the one-dimensional case is, in effect, identical to Theorem 2.2 since, in that case, the area of the nuclear membrane is not related to the size of the cell and changes in cell size are equivalent to changes in the diffusion rates.

## 3. CONCLUSIONS

The model that we have presented and analyzed for the triggering of the $S$ phase is based on the accepted mechanism of biosynthetic control by repression due to Jacob and Monod [5] and on simple physical considerations concerning the cell's size, shape and internal organization. The use of two distinct compartments in the model is supported both by the physical organization of eukaryotic cells and by experimental evidence of the importance of compartments in the cell [16]. The mathematical analysis of this model that we have carried out so far indicates that the proposed triggering mechanism is in qualitative agreement with the observed behavior of the cell cycle under variations of different pertinent parameters. It remains, however, to yet analyze the effects of shape, the proximity of other cells which can change the shape of a cell due to mechanical forces, and the implications that our proposed mechanism has on the behavior of synchronized populations of dividing cells. We are currently pursuing each of these questions by doing either further mathematical analysis of extensions of our model or by large scale numerical computations whenever the complexity of the model does not allow strict analytical results to be established. In particular, for cell shapes that do not have simple geometric symmetries, as did the centrally symmetric spherical cells we have discussed in the main body of the paper, we are currently performing numerical integrations of the equations of our model for various parameter ranges. This numerical work requires considerable computer resources and is being done on a large parallel processor (the Cray 1 XMP at the Supercomputer Center in San Diego) with the support of the National Science Foundation. As the results of these computations become available we will be able to compare division times of cells that are spherically shaped with those that are flattened and see how they correlate with available experimental information. We shall also be able to study the effects of environmental changes by the addition of external fluxes at the boundary of the outside cell wall. We are also developing a mathematical theory for the study of large ensembles of synchronized cells each of which is dividing according to the triggering mechanism we have proposed. This will allow us to compare the predictions of our model with the available data on *$\alpha$-curves* and *$\beta$-curves* [1, 11, 12] for such synchronized populations. We also note that the current type of compartmental reaction diffusion model can be easily extended to include large chains of enzyme catalyzed reactions, other methods of biosynthetic control (positive feedback or induction, for example), and more that two compartments. We have already studied some of these extensions and our work [8] includes the analysis of a three compartment model. We will pursue these extensions if the work on the effects of cell shape variation and on ensembles of synchronized cells leads to good agreement with available experimental observations.

We finally note that the type of compartmental model we have presented here with interactions via transfer through the boundaries of the compartments has applications to a variety of physiological processes. In particular, there are implications concerning the adequacy of using well-mixed compartmental models to describe some of these processes as illustrated by our results for the three compartment reaction-diffusion model described in Ref. [8]. Also, as we have shown, it is possible to use appropriate time delays to model the effects of spatial diffusion in such models. However, the delayed terms are certainly not as simple as was previously thought [15], and depend in an intricate way on the parameters of the model as well as on the size and shape of the cell as is discussed in Refs [7, 8]. This is an area that we have barely touched upon to date and plan to study systematically in the future.

*Acknowledgements*—The work of the first author was partially supported by NSF Grant No. DMS-8703631 and that of the second author by NSF Grant No. DMS-8683787.

## REFERENCES

1. B. Alberts, D. Bray, J. Lewis, M. Raff, K. Roberts and J. D. Watson, *Molecular Biology of the Cell*. Garland Publishing, New York (1983).
2. A. T. Winfree, *The geometry of Biological Time*, *Biomathematics*, Vol. 8. Springer, New York (1980).
3. B. C. Goodwin, Oscillatory behavior of enzymatic control processes. *Adv. Enzyme Reg.* **3**, 425–439 (1965).
4. B. C. Goodwin, *Temporal Organization in Cells*. Academic Press, New York (1963).
5. F. Jacob and J. Monod, On the regulation of genome activity. *Cold Spring Harbor Symp. Quant. Biol.* **26**, 193–211, 389–401 (1961).
6. H. T. Banks and J. M. Mahaffy, Mathematical models of protein synthesis. Technical Report, Division of Applied Mathematics, Lefshetz Center for Dynamical Systems, Providence, R.I. (1979).
7. S. N. Busenberg and J. M. Mahaffy, The effects of dimension and size for a compartmental model of repression. *SIAM Jl Appl. Math.* (in press).
8. S. N. Busenberg and J. M. Mahaffy, Interaction of spatial diffusion and delays in models of genetic control by repression. *J. Math. Biol.* **22**, 313–333 (1985).
9. J. M. Mahaffy and C. V. Pao, Models of genetic control by repression with time delays and spatial effects. *J. Math. Biol.* **20**, 39–57 (1984).
10. J. J. Tyson, Periodic enzyme synthesis and oscillatory repression: Why is the period of oscillation close to the cell cycle time? *J. theory. Biol.* **103**, 313–328 (1983).
11. A. Lasota and M. C. Mackey, Globally asymptotic properties of proliferating cell populations. *J. Math. Biol.* **19**, 43–62 (1984).
12. M. C. Mackey, A deterministic cell cycle model with transition probability behavior. In *Temporal Order* (Eds L. Renzigand and N. I. Jaege), pp. 313–328. Springer, Berlin (1985).
13. W. Alt and J. J. Tyson, A stochastic model of cell division (with application to fission yeast). Preprint (1986).
14. J. M. Mahaffy, A test for stability of linear differential delay equations. *Q. appl. Math.* **40**, 193–202 (1982).
15. N. MacDonald, Time lag in biological models. *Lecture Notes Biomath.*, Vol. 27. Springer, Berlin (1978).
16. W. G. Dunply and J. E. Rothman, Compartmental organization of the golgi stack. *Cell* **42**, 13–21 (1985).